Cerebral Venous and Dural Sinus Thrombosis*

State-of-the-Art Imaging

Jennifer Linn, Hartmut Brückmann[1]

Abstract
Cerebral venous and sinus thrombosis (CVST) constitutes a rare but important cause of stroke. It occurs in all age groups, but affects predominately young and middle-aged females. Three subtypes of CVST can be differentiated: sinus thrombosis (ST), deep cerebral venous thrombosis (DCVT), and cortical vein thrombosis (CVT). Both DCVT and CVT can present either in isolated forms or – more often – in combination with an ST. The symptoms of CVST are highly variable, thus, diagnosis is often made with a considerable delay.
This review first presents a short summary of the epidemiology, risk factors, clinical signs, and prognosis of CVST. Then, the authors focus on the neuroradiologic diagnosis of this disease, and give an overview of the diagnostic value of magnetic resonance imaging (MRI), computed tomography (CT), and CT angiography (CTA) for CVST.

Key Words: Sinus thrombosis · Deep cerebral venous thrombosis · Cortical vein thrombosis · Imaging · MRI · CTA

Clin Neuroradiol 2010;20:25–37
DOI 10.1007/s00062-010-9035-7

Zerebrale Sinus- und Hirnvenenthrombose. Aktuelle Bildgebung

Zusammenfassung
Die zerebrale Sinus- und Hirnvenenthrombose (CVST) stellt eine seltene, aber wichtige Schlaganfallursache dar. Sie kann in allen Altersgruppen auftreten, Frauen jüngeren bis mittleren Alters sind jedoch gehäuft betroffen. Drei Unterformen der Erkrankung können unterschieden werden: die Sinusthrombose (ST), die innere Hirnvenenthrombose (DCVT) und die Thrombose der kortikalen Venen (CVT). Sowohl die DCVT als auch die CVT treten entweder isoliert oder – deutlich häufiger – in Kombination mit einer ST auf. Die Symptome einer CVST sind sehr variabel, was dazu führt, dass die Diagnose häufig erst mit einer deutlichen Verzögerung gestellt wird.
Dieser Übersichtsartikel liefert eine kurze Zusammenfassung der Epidemiologie, der Risikofaktoren, der Klinik und der Prognose der CVST. Der Schwerpunkt der Arbeit liegt auf der neuroradiologischen Diagnose der Erkrankung. Die diagnostische Wertigkeit der Magnetresonanztomographie (MRT), der Computertomographie (CT) und der CT-Angiographie (CTA) wird dargestellt.

Schlüsselwörter: Sinusthrombose · Innere Hirnvenenthrombose · Thrombose der kortikalen Venen · Bildgebung · MRT · CTA

Introduction

Cerebral venous and dural sinus thrombosis (CVST) is a rare but important cause of stroke. In Europe, it accounts for < 1% of all strokes [1, 2], with an estimated annual incidence of CVST of 3–4 cases per million in adults and 7 cases per million in children and neonates [3]. Although CVST can occur in all age groups, young and middle-aged patients (< 40 years of age) are most commonly affected, with a female predominance [4]. An abundance of predisposing factors or direct causes of CVST have been identified. The most important ones are a prothrombotic state, either genetically imposed or

*Dedicated to Professor Armin Thron, MD, on the occasion of his 65th birthday.

[1]Department of Neuroradiology, University Hospital Munich, Germany.

Received: November 14, 2009; revision accepted: January 26, 2010
Published Online: February 28, 2010

acquired, an intake of oral contraceptives, last trimester of pregnancy, puerperium, and ear, nose and throat (ENT) infections [1, 5, 6]. In > 40% of patients two or more risk factors can be found, while in about 15–20% of all CVST cases no risk factor can be identified [5].

Subtypes of Cerebral Venous and Sinus Thrombosis

Depending on the involved venous structures, three subtypes of CVST can be differentiated. They differ not only with regard to their clinical presentation and their prognosis, but also with regard to the most appropriate imaging.

Sinus Thrombosis

A sinus thrombosis (ST) indicates a thrombotic occlusion of one or more dural sinuses. It is the most common form of CVST, and typically involves the superior sagittal sinus, followed by the transverse sinus [5].

Deep Cerebral Venous Thrombosis

A deep cerebral venous thrombosis (DCVT) is defined as a thrombosis of the deep cerebral veins (i.e., the internal cerebral veins, the great vein of Galen, and/or the basal veins of Rosenthal, and their tributaries). Rarely it occurs as an isolated form, i.e., without the involvement of a sinus. More often, a combination with an ST is present. In literature on DCVT the straight sinus often is classified as belonging to the deep cerebral venous system [7]. An involvement of the deep cerebral veins (i.e., the internal cerebral veins, the basal veins of Rosenthal, and their tributaries) is found in approximately 10% of patients with CVST [8, 9].

Cortical Vein Thrombosis

The term cortical vein thrombosis (CVT) denotes a thrombosis of one ore more cortical veins. Similar to DCVT, isolated forms which are rather rarely diagnosed, must be distinguished from combined CVTs [10–12]. These combined forms additionally involve one or more sinuses, typically the superior sagittal sinus. This is due to the fact that they usually develop secondary to an ST via retrograde thrombus propagation from the occluded sinus [10]. A CVT most commonly affects the frontal cortical veins, followed by the parietal veins [13]. Isolated CVTs of the anastomotic vein of Labbé have also been reported [10]. Compared to the sinuses and the deep cerebral veins, the cortical veins are highly variable in number, size, and localization [14]. This – and the fact that an established gold standard for this diagnosis is still lacking – hampers their radiologic evaluation [15]. Thus, isolated CVTs have mostly been described in case reports or in small series [10, 16–21]. Yet, more recently, with the advent of modern magnetic resonance (MR) techniques (see below), more and more cases are being reported, raising the suspicion that isolated CVTs indeed are more common than previously thought [11, 12, 22–24].

Clinical Signs and Symptoms of Cerebral Venous and Sinus Thrombosis

In contrast to arterial strokes, symptoms in CVST often develop subacutely [25–27]. The clinical presentation of a CVST is highly variable and largely depends on both the localization and the extent of the thrombosis [3]. Besides these important factors, patient's age [28, 29], the presence of a parenchymal involvement, and the interval from symptom onset to diagnosis [30] are important factors for the clinical presentation of a CVST [11, 31]. Severe headache often constitutes the first symptom, occurring in approximately 75–90% of all patients; however, the specificity of this symptom is low [8]. In addition to headache, patients often present with other signs and symptoms of an elevated intracranial pressure, namely dizziness, nausea, and visual disturbances [32, 33]. Furthermore, focal neurologic deficits including cranial nerve palsies or seizures are found [8, 15]. CVST should always be considered as a potential differential diagnosis in young and middle-aged patients with unusual or severe headache or with stroke-like symptoms in the absence of the common vascular risk factors, in patients with intracranial hypertension, and in patients with evidence of hemorrhagic infarcts on computed tomography (CT).

An involvement of the deep cerebral veins or of the cortical veins has a major impact on clinical presentation. The symptoms of DCVT are highly variable, with headache (> 80%) and reduced consciousness (> 70%) being most frequently observed [34]. In CVT, focal or generalized seizures, and hemiparesis, aphasia, hemianopia or other focal deficits, are common, and occur often without signs of elevated intracranial pressure [10, 15].

Normal D-dimer levels have a high negative predictive value in patients with suspected CVST [35]. However, it can be normal in up to 25% of cases [34, 36]. These false-negative results might be due to the relatively small thrombus volume, especially in patients with an isolated DCVT [34].

Prognosis and Outcome

Due to a greater awareness of the disease, improved neuroimaging techniques, and more effective treatment options, the outcome of CVST significantly improved in the past decades. If diagnosed promptly, there is a good prognosis with restitutio ad integrum in 80% of cases [1]. Yet, despite modern imaging techniques, the average diagnostic delay is still 7 days, and might be even longer in patients with DCVT, in male patients, or in patients presenting with an isolated intracranial hypertension syndrome [3, 34, 37]. This is due to the wide clinical spectrum and the lingering or subacute onset, especially in the small portion of patients with normal D-dimer levels. Thus, in a subset of about 10–15% of patients there is a poorer outcome. In addition to delayed diagnosis [36], the following risk factors are associated with a poor prognosis: higher age, male gender, hemorrhage, involvement of the deep cerebral veins and of the right transverse sinus, and the presence of central nervous system infections or neoplasms [1, 8, 38].

As mentioned above, the involvement of the deep veins has been shown to be a risk factor for death and long-term sequelae [8, 9]. Yet, in a recent study by Pfefferkorn et al. on 32 patients with DCVT, the outcome was better than previously reported: 75% of patients improved on intravenous heparin or subcutaneous low-molecular-weight heparin therapy. Yet, eight patients, six of which received local endovascular therapy, deteriorated with progressing coma. Two of those patients died. The presence of an additional sinus involvement did not influence the outcome in this study [34].

Imaging

Direct Signs Versus Indirect Signs

Regardless of its localization, CVST can present with both direct and indirect imaging signs. The term *direct signs* refers to findings regarding an occluded vessel itself, while *indirect signs* indicate concomitant changes of the brain parenchyma.

Direct signs include the *positive* visualization of the thrombotic material within a respective vein or sinus on

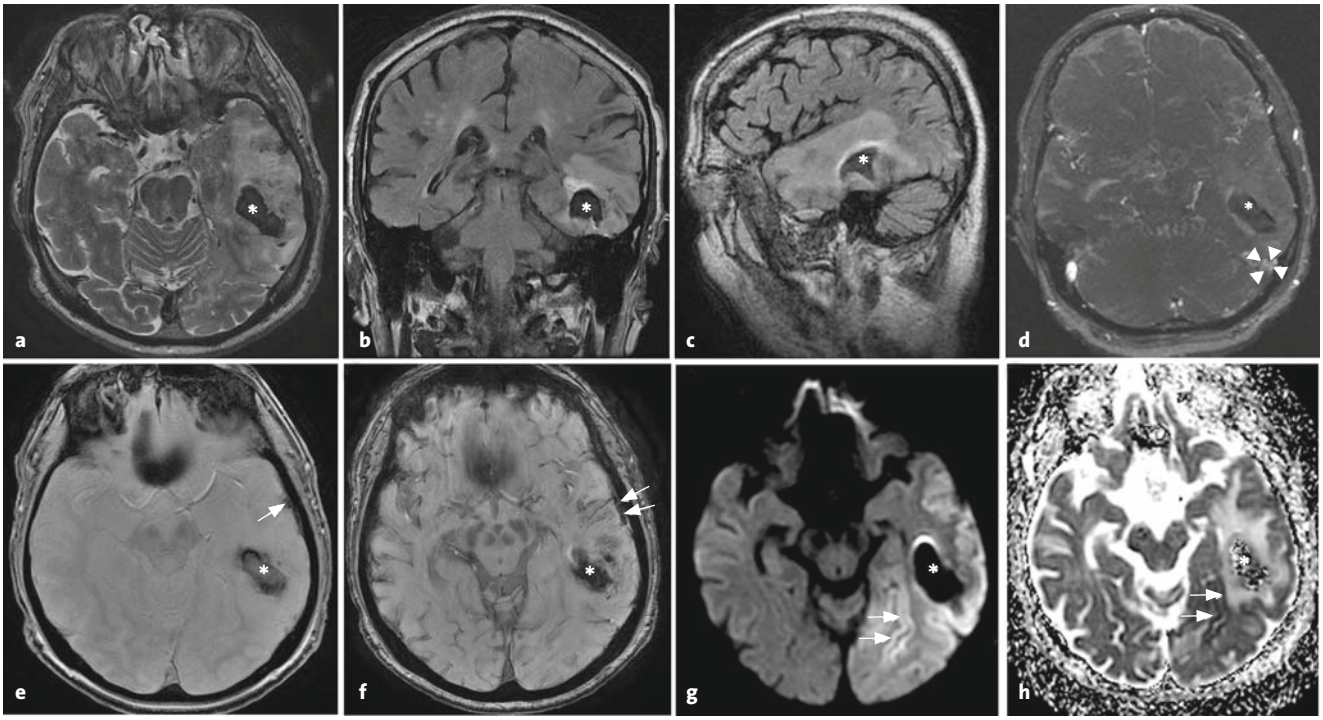

Figures 1a to 1h. 31-year-old male patient with CVST involving the superior sagittal sinus (not shown), the proximal part of the right transverse sinus (not shown), the left transverse sinus (arrowheads in d), and the left anastomotic vein of Labbé (arrows in e and f). MRI performed on day 3 after symptom onset demonstrates left temporal edema, hyperintense on T2- (a) and FLAIR-weighted images (b: coronal, c: sagittal), and hemorrhage, hypointense on all sequences (asterisk). On T2*-weighted image (e) and on susceptibility-weighted sequence (SWAN, f) the thrombus within the left anastomotic vein of Labbé is directly visualized as hypointense clot (arrows in e and f). DWI (g: B1000 image; h: ADC map) depicts diffusion restriction indicative of cytotoxic edema within part of the affected brain region (arrows in g). There is no flow signal within the left transverse sinus of the source image of venous TOF-MRA (arrowheads in d).

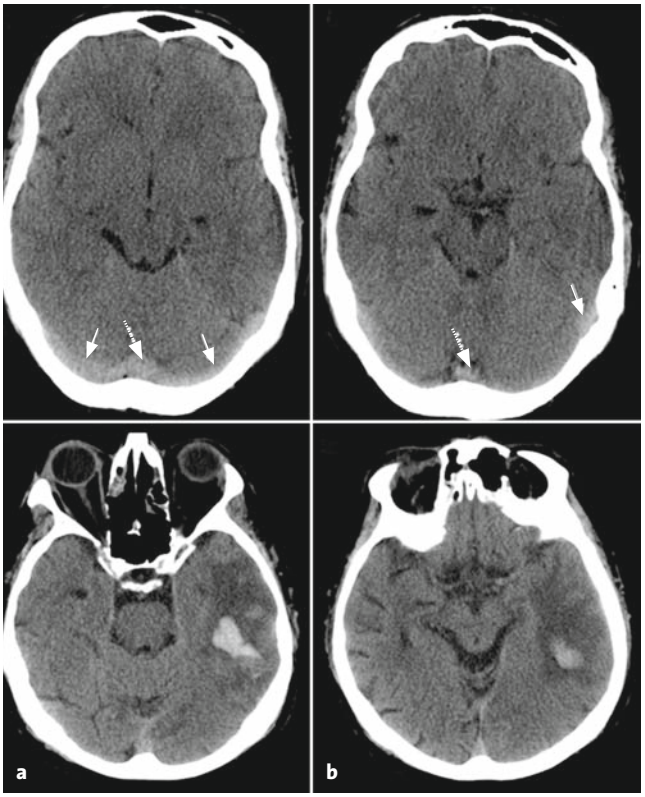

Figures 2a and 2b. NECT scans of the same patient as shown in Figure 1. On initial imaging, performed at day 1 after symptom onset (a, b), a cord sign is present within the superior sagittal sinus (dotted arrows) and both transverse sinuses (normal arrows). Neither hemorrhage nor edema are present. Follow-up imaging on day 3 reveals left temporal edema and hemorrhage as indirect signs of CVST. Based on these CT findings, MRI (shown in Figure 1) was initiated.

nonenhanced CT (NECT) or magnetic resonance imaging (MRI), as well as the *negative* identification of the thrombus either as a contrast filling defect (on digital subtraction angiography [DSA], CT angiography [CTA], or on other contrast-enhanced images) or as a lack of flow signal (on a flow-sensitive venous MR angiography [MRA]).

Venous edema or infarction, as well as subarachnoid or parenchymal hemorrhages represent the *indirect* imaging signs of CVST on CT and MR. In ST or CVT the edema typically does not follow the borders of arterial territories, and is often located adjacent to the surface of the brain (Figures 1 and 2). On the contrary, a DCVT results in unilateral or, more commonly, bilateral venous edema or infarction of the thalami and basal ganglia [7, 39] (Figure 3). The presence of a parenchymal hemorrhage at the time of diagnosis of a CVST has been shown to be associated with a more severe clinical presentation at onset and a worse outcome [8, 9].

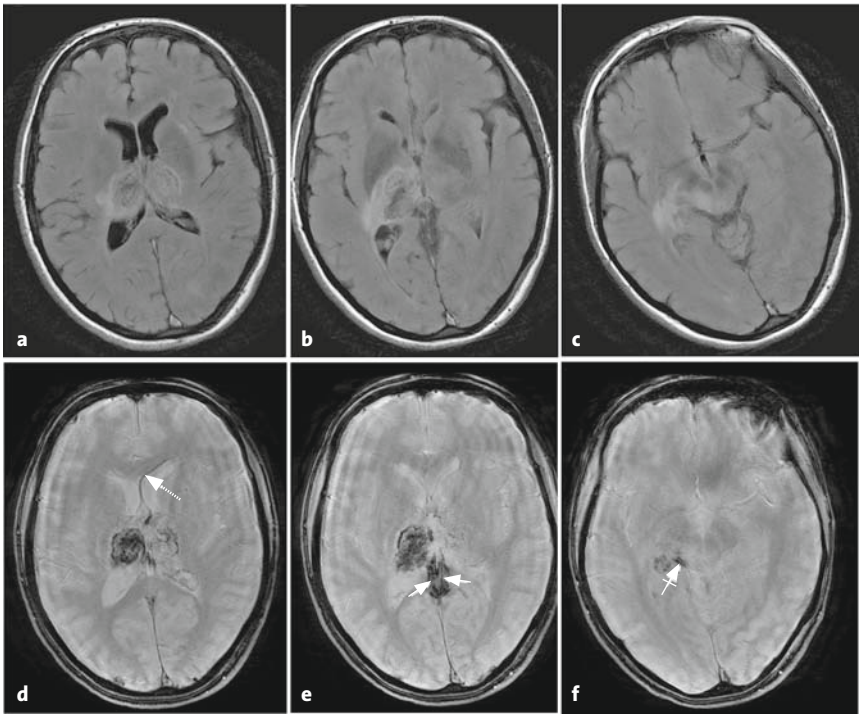

Figures 3a to 3f. 38-year-old female patient with combined DCVT. FLAIR images (a–c) and T2*-weighted images (d–f) show bilateral thalamic edema, predominately on the right side. T2*-weighted images reveal the hypointense clot in the left septal vein (dotted arrow in d), both internal cerebral veins (normal arrows in e), and the right basal vein of Rosenthal (crossed arrow in f).

Digital Subtraction Angiography

Traditionally, DSA was the gold standard for the diagnosis of a CVST, but it has nowadays been widely replaced by MRI and CTA [1, 3, 15, 40–42]. To date, DSA is no longer a routine component of the diagnostic work-up in CVST in most institutions, but is reserved for cases in which an interventional therapy, e.g., a local thrombolysis, is considered [3, 32, 34]. Compared to MRI and CTA, DSA still is superior with regard to spatial and temporal resolution and offers precise dynamic information on collateral venous drainage, which might be helpful in a subset of unclear cases (Figure 4). With regard

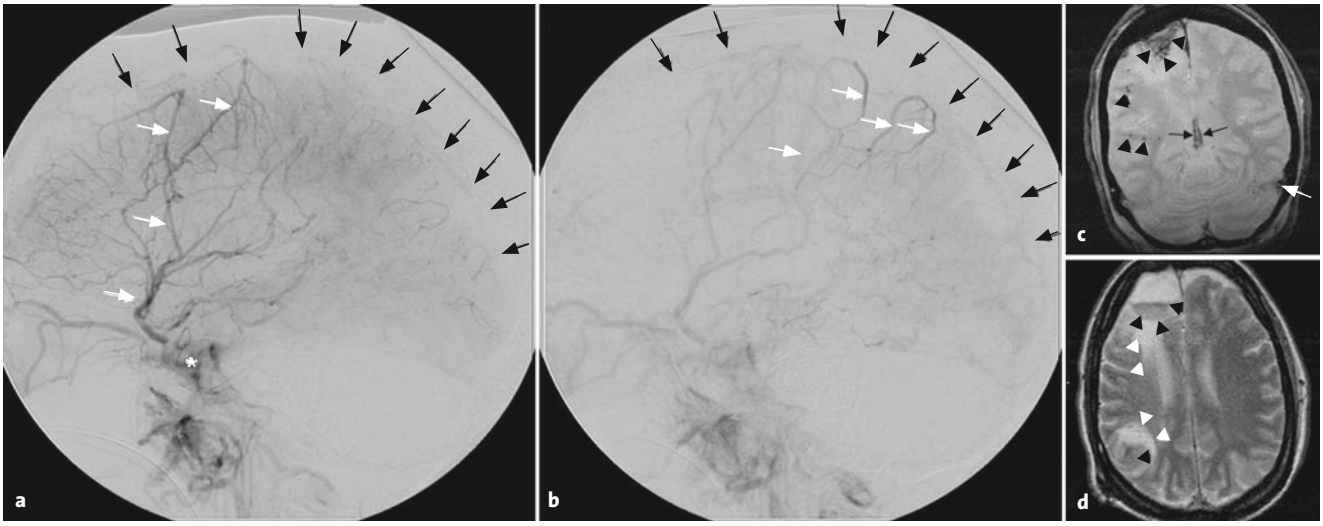

Figures 4a to 4d. 29 year-old-female patient with an extensive CVST involving the superior sagittal sinus, the left transverse sinus (white arrow in c), and the internal cerebral veins (black arrows in c). a, b) DSA, sagittal view, venous phases after selective catheterization of the left internal carotid artery. c) T2*-weighted image performed in an oblique coronal orientation. d) Axial T2-weighted image. DSA (a, b) shows a collateral, delayed venous drainage via the cortical veins (white arrows in a and b), and the cavernous sinus (asterisk in a). This example illustrates the value of DSA for the evaluation of flow dynamics in CVST. The black arrows in a and b indicate the course of the occluded superior sagittal sinus. T2*- (c) and T2-weighted images (d) reveal right frontal and right parietal edema (white arrowheads in d) with hemorrhage (black arrowheads in c and d).

to CVT, some authors still discuss whether DSA has a higher sensitivity compared to the other modalities [11], but systematic data in literature to support this hypothesis is lacking. In case of an isolated CVT, DSA can show a "missing" cortical vein, and/or a partially visualized vein which abruptly stops or is surrounded by dilated cortical veins [11, 43]. Yet, the value of these signs is limited by the high intra- and interindividual variability of both the number and location of the cortical veins [14]. Thus, the DSA diagnosis of a CVT predominately relies on the following *indirect* imaging signs: a delayed focal venous drainage, evidence of vascular congestion in the parenchyma, which is drained by the occluded vein, and the presence of cortical collaterals appearing as "corkscrew vessels" [11, 43]. The above-mentioned drawbacks of DSA concerning the cortical veins likewise apply to all other angiographic techniques, including CTA and MRA.

Magnetic Resonance Imaging

MRI represents the current gold standard for CVSTs [1, 3, 15, 40, 41], and is the method of choice in the diagnostic arms of large international trials on this entity [3, 5]. Yet, there is emerging evidence that CTA is at least equally sensitive for ST compared to MRI [1] (see below).

Direct CVST Signs on MRI

On MRI, the thrombotic material shows rather complex signal intensity characteristics, which do depend on the stage of the thrombosis (hyperacute, acute, subacute, or chronic stage) and on the imaging sequence which is used [11, 25, 41, 44]. They apply likewise to ST, DCVT, and CVT [10, 11, 13]. Detailed knowledge on this time-dependent signal course is required to interpret the MR signal of a CVST correctly.

Spin-Echo Sequences

In the acute phase of a CVST, i.e., on days 0–5 from symptom onset, the thrombus typically shows a hypointense signal on T2-weighted spin-echo images and an isointense signal on a T1-weighted spin-echo sequence [11, 41, 44, 45]. Thus, it can only poorly be distinguished from normal flow signal within the vessels. This limits the sensitivity of these sequences especially during the early days of a CVST [11, 41, 44, 46]. After approximately 5 days, thus in the subacute phase (days 6–15), the clot becomes more and more hyperintense on both T2- and T1-weighted images [11, 44, 45]. On fluid-attenuated inversion-recovery (FLAIR) and proton density (PD) sequences, the clot appearance is widely similar compared to that on T2-weighted spin-echo sequences [13] (Figures 5 and 6). Although the above-mentioned signal characteristics are true for the majority of cases,

there are considerable variations in a significant proportion of cases (Table 1).

Due to this complex signal course, the interpretation of MRI in CVST requires expert knowledge to avoid potential diagnostic and technical pitfalls [25, 41]. For example, hyperintense signal resulting from regular flow in T1-weighted images performed without adequate flow compensation might simulate a thrombus as shown in Figure 7. This underlines the challenge radiologists are faced with in interpreting MR sequences for venous system thrombosis, and represents a certain drawback compared to CT, which is easier to obtain and to interpret.

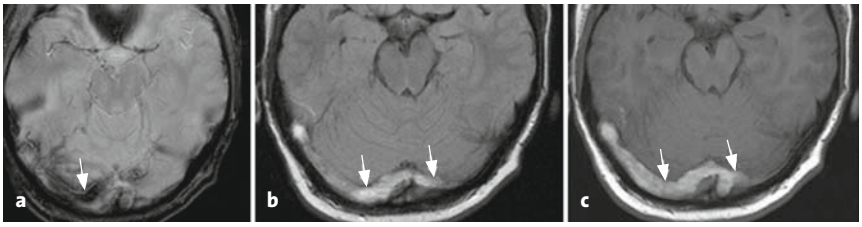

Figures 5a to 5c. MRI performed in the subacute phase (8 days after symptom onset) in a patient with thrombosis of both transverse sinuses (arrows), the confluens sinuum, and the superior sagittal sinus (not shown). The thrombotic material shows a hypointense signal on T2*-weighted sequence (a), and a hyperintense signal on both FLAIR (b) and T1-weighted (c) images.

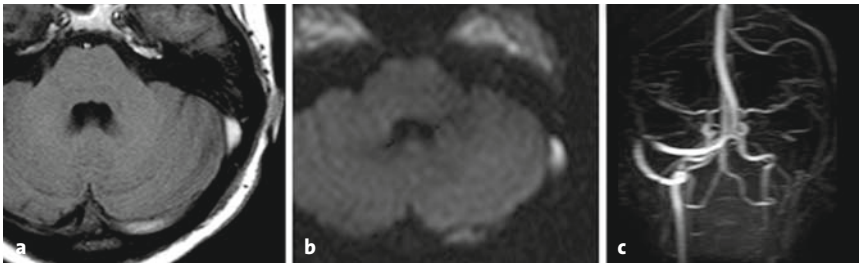

Figures 6a to 6c. 42-year-old female patient with a subacute CVST of the left transverse sinus. The clot is hyperintense on the B1000 DWI. a) FLAIR; b) DWI (b-value 1,000); c) venous TOF-MRA.

Diffusion-Weighted Imaging

In some CVST cases, the intravasal clot shows a diffusion restriction with a hyperintense signal on diffusion-weighted imaging (DWI) with a b-value of 1,000 and a lowered apparent diffusion coefficient (ADC) value [45, 47, 48]. This finding has predominately been described in subacute cases with a hyperintense thrombus signal on FLAIR- and T1-weighted images [45, 47] (Figure 6). Its sensitivity varies from approximately 4% to 40% [45, 47, 48]. There is evidence that the presence of a hyperintense clot on DWI might be of prognostic value for potential recanalization of occluded vessels [47].

T2-Weighted Gradient-Echo Sequence*

In recent years, T2*-weighted images have been shown to be of great value in CVST [11, 13, 19, 20, 45, 49, 50]. This is especially true in the acute phase of the disease, when the thrombus is still isointense on T1-weighted images [45, 49]. On T2*-weighted images, the thrombus is directly visualized as a profound, homogeneous hypointense tubular structure, showing a so-called blooming, during the first days of a CVST (Figures 1, 3, 5, 8, and 9). While results regarding the hypointense clot signal on this sequence are very consistent for acute thrombosis, there are somewhat divergent results regarding the time course of the signal. Some authors observed a relatively strong time dependence of the hypointensity, which was present in 90% of cases during the first weeks but in only 9% and 32% in the subacute and chronic phases, respectively [50]. Yet, in other studies hypointensity on T2*-weighted sequences has been shown to be positive up to 1 year after symptom onset [11, 45], and was present in > 30% of cases on 4-month follow-up imaging [45]. The sequence is particularly useful in CVT, where it has been shown to be superior to all other

Table 1. Variability of clot signal characteristics on T1- (T1w) and T2-weighted spin-echo sequences (T2w) in relation to the stage of the disease. FLAIR: fluid-attentated inversion-recovery sequence; MR: magnetic resonance; PD: proton-density-weighted sequence. Note that numbers printed in bold indicate the most common clot signal intensity in the respective stage.

MR sequence	Signal intensity	Acute stage (0–5 days)[b]	Subacute stage (6–15 days)[b]	Chronic stage (> 15 day)[b]
T1w	Hyperintense	30%	**71%**	39%
	Isointense	**68%**	29%	**54%**
	Hypointense	2%	0%	7%
T2w[a]	Hyperintense	25%	**52%**	**43%**
	Isointense	10%	32%	**45%**
	Hypointense	**65%**	16%	12%

[a] Signal characteristics indicated for T2w apply equally to FLAIR and PD
[b] refers to days from symptom onset

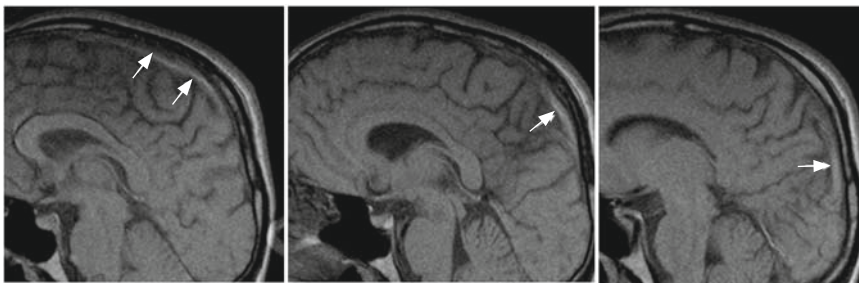

Figure 7. Sagittal T1-weighted images in a healthy volunteer depict hyperintense flow signal in the normal superior sagittal sinus as a potential pitfall. To avoid this artifact, the sequence should be performed with adequate flow compensation.

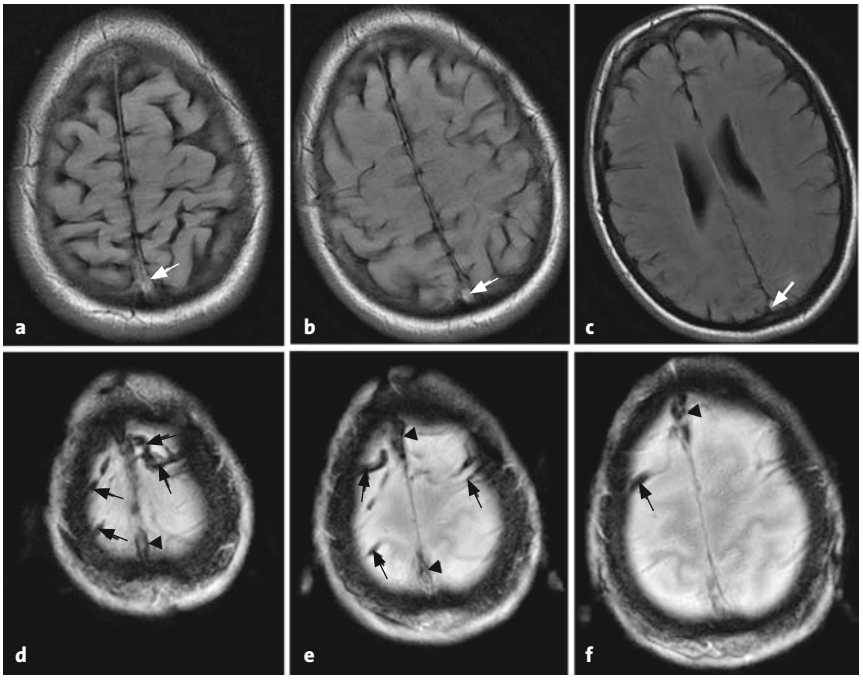

Figures 8a to 8f. CVT with involvement of the superior sagittal sinus. FLAIR images (a–c, arrows) depict the hyperintense clot within the superior sagittal sinus (arrowheads), while the affection of the cortical veins is best seen on T2*-weighted images (d–f, arrows).

sequences (Figures 1 and 8). Based on the available data in literature, we strongly recommend to consider the T2*-weighted sequence as the present gold standard for the diagnosis of an isolated or combined CVT and for the exclusion of a cortical vein involvement in ST. It should be added as a standard sequence for routine imaging protocols for CVST.

To avoid false-positive results of T2*-weighted imaging, a linear hypointense signal should only be interpreted as indicative of a venous thrombosis, if it is prominent ("blooming phenomenon"), tubular, shows a round diameter on slices perpendicular to its course, and encompasses a vessel lumen [11, 13, 45]. Chronic subarachnoid hemorrhage or focal superficial siderosis, which is defined as a hypointense linear signal within the superficial layers of the cortex, should not be mistaken for a hypointense clot (Figure 10). The latter is typically found in patients with cerebral amyloid angiopathy, or in vasculitis [51].

In recent years, susceptibility-weighted sequences, which are even more sensitive compared to conventional T2*-weighted sequences, are used to depict the cerebral venous anatomy with great detail. They are based on different acquisition and/or postprocessing techniques and are known as, e.g., SWI (susceptibility-weighted imaging) or SWAN (susceptibility-weighted angiography) [52, 53] (Figure 11). Their application in a very limited number of CVST cases yielded promising initial results [54] (Figure 1). Yet, care has to be taken, as both normal, and occluded veins appear hypointense on these sequences. Thus, systematic studies are needed to test the value of this technique for CVST.

Venous MRA Techniques

Different MRA techniques are available for the evaluation of the cerebral venous vasculature. Venous time-of-flight (TOF) MRA is most commonly used in clinical routine conditions [11, 19] (Figure 6). To avoid misinterpretation of a venous TOF-MRA, the following potential pitfalls have to be considered: (1) artificial flow gaps on TOF-MRA can either result from slow blood flow or from in-plane flow. Flow gaps within the non-dominant transverse sinus (typically the left one) are present in > 30% of patients [40, 55]. (2) A hypo- or aplastic (left) transverse sinus could be misinterpreted as a thrombosis, if MRA is interpreted solely [41, 55] (Figure 12), and (3) a subacute, hyperintense thrombus might simulate flow in this sequence [40]. With regard to the evaluation of the cortical veins, venous MRA suffers from the same limitations as DSA and CTA,

namely the considerable anatomic variations of these vessels [13].

In addition to TOF-MRA, phase-contrast- as well as contrast-enhanced venous MRA, and MPRAGE (magnetization-prepared rapid-acquisition gradient-echo) techniques are in use to investigate the cerebral veins and sinuses [56–58]. Yet, data on their value for CVST is limited [56]. Furthermore, there exist new, promising MRA techniques such as time-resolved MRA [59, 60], which might further improve the value of MR for the evaluation of the cerebral veins and sinuses. A very recent study on 20 CVST patients and 19 controls demonstrated that the combination of a dynamic and a static three-dimensional combined MR venography – the so-called *combo 4-D MRV* – was superior to TOF-MRA [61]. Future studies should address the potential value of these sequences as well as the impact of higher field strengths for the diagnosis of CVST.

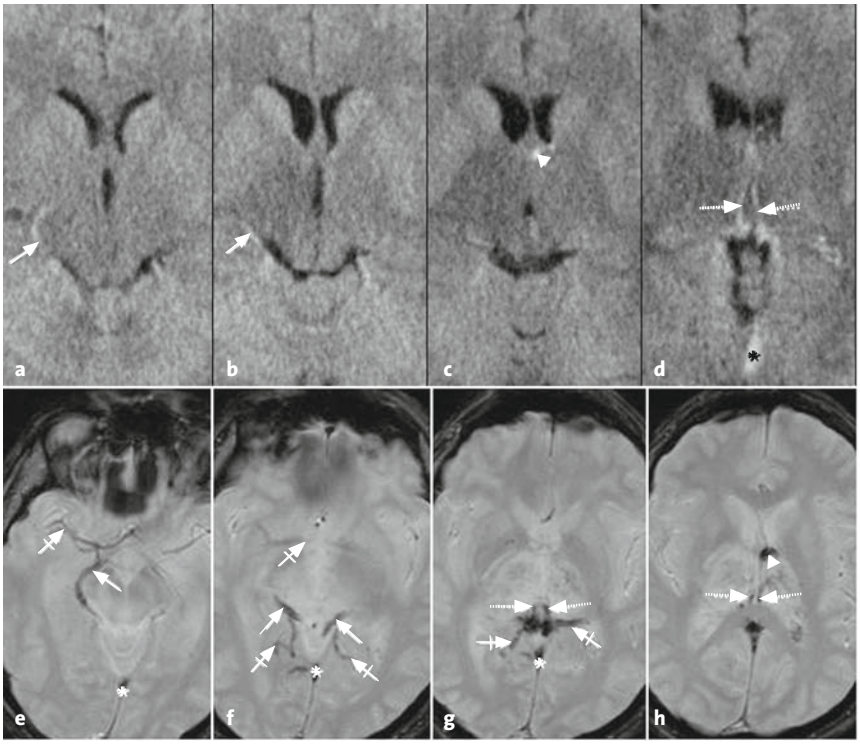

Figures 9a to 9h. DCVT involving both internal cerebral veins (dotted arrows), both basal veins of Rosenthal (normal arrows), and their tributaries (see, for example, crossed arrows), the left thalamostriate vein (arrowheads), and the straight sinus (asterisks). The thrombotic material is profoundly hyperdense on NECT (a–d), and hypointense on T2*-weighted images (e–h).

Indirect Signs of CVST on MRI

MRI represents the gold standard also for the visualization of secondary parenchymal changes in CVST [31, 62]. T2-weighed, PD-weighted or FLAIR images best depict venous edema and infarction, while T2*-weighted images are superior with regard to associated hemorrhages (Figures 1 and 3).

DWI shows variable signal intensities in CVST. Both cytotoxic as well as vasogenic edema can be present [63, 64] (Figure 1). There is evidence from both patient and animal model studies that cytotoxic edema precedes vasogenic edema in CVST. This is indicated by a decreased ADC at very early stage, which is followed by a normalization or increase thereafter [65].

Computed Tomography

NECT

In most clinical institutions, NECT is still the method of first choice in neurologic disorders, especially in the emergency setting. This is mostly due to its wide availability, its cost-effectiveness and short examination time, as well as to the fact that it depends less on patient cooperation compared to MRI. On NECT, a newly formed thrombus shows a homogeneous, hyperattenuating signal within the affected vessels [7, 66, 67] (Figures 2, 9, and 13). This direct sign of CVST is called *cord sign* or *dense vein sign*. Both items are used inconsistently for both veins and sinuses in literature [7, 66, 67]. We prefer to apply the term cord sign for sinuses

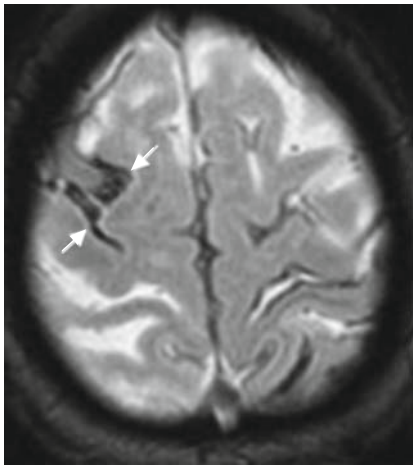

Figure 10. The T2*-weighted image depicts bilateral superficial siderosis (see, for example, arrows) in a patient with histopathologically proven cerebral amyloid angiopathy. Such a finding should not be misinterpreted as cortical venous clot.

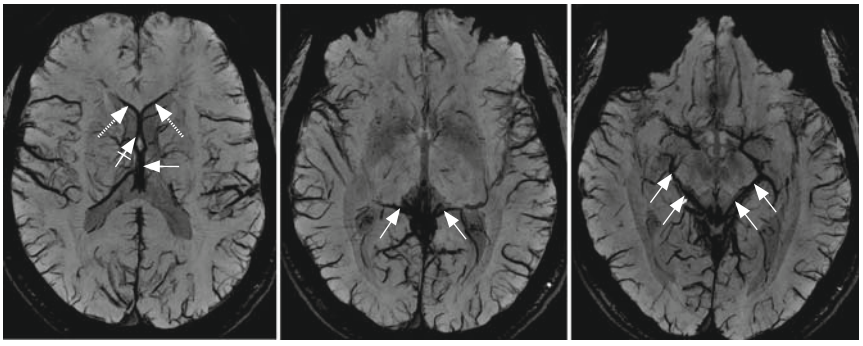

Figure 11. SWAN depicts the cerebral veins in great detail: the septal veins (dotted arrows), the thalamostriate veins (crossed arrow), the internal cerebral veins (thin arrow), and the basal veins of Rosenthal (thick arrows).

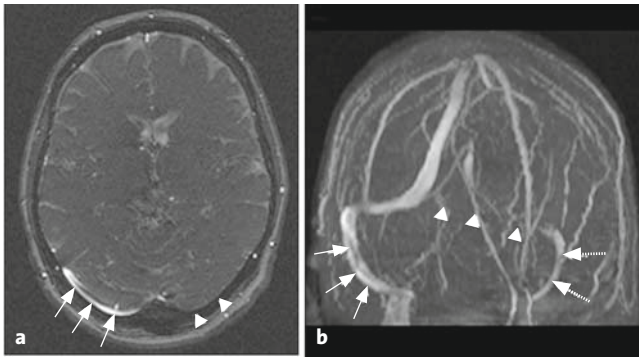

Figures 12a and 12b. Potential pitfall on venous TOF-MRA (a: source image; b: maximum intensity projection) of a healthy volunteer: aplastic proximal left transverse sinus (arrowheads), hypoplastic left sigmoid sinus (dotted arrows in b), and normal right transverse sinus (normal arrows in a and b).

and dense vein sign for veins [7]. This hyperdense appearance of the clot is best seen within the 1st week of the disease. After 7–14 days, the thrombus becomes first iso- and later hypodense [66]. With regard to the sinuses, the sensitivity of the cord sign has been found to be rather low (25–65%) [7, 67]. The same seems to be true for the cortical veins [13]. Thus, NECT alone does not allow the confident diagnosis or exclusion of an ST or a CVT.

In contrast to this, the dense vein sign has a very high sensitivity (100%) and a high specificity (> 99%) both for the overall diagnosis of an isolated or combined DCVT, as well as for the correct detection of the individually affected deep cerebral veins [7] (Figure 9). Furthermore, the interobserver agreement regarding the presence of a dense vein sign is excellent in DCVT, and the diagnostic confidence for this entity is high if this sign is present [7]. These findings indicate that NECT is very helpful in the diagnosis of DCVT.

With regard to the detection of parenchymal changes, i.e., indirect signs of CVST, MRI is superior to NECT. Yet, NECT also reaches acceptable high sensitivity and specificity values for these sequelae of CVST [7, 13, 42] (Figure 2).

Potential pitfalls on NECT can result in both false-positive and false-negative results. Partial volume effects, caused by adjacent bony structures, can lead to false-positive cord signs and dense vein signs [68] (Figure 14). This is especially true for the sinuses and the cortical veins, which are located in immediate vicinity to the skull, while the deep cerebral veins are much less prone to these artifacts due to their localization [7]. In addition, normal flowing venous blood can also appear mildly hyperdense on NECT, probably due to high hematocrit values [55, 66]. A possible explanation for false-negative hyperdense sinuses in ST might be the less severe clinical presentation of a thrombosis of one sinus (e.g., the transverse sinus) compared to that of DCVT. If imaging is not performed immediately after symptom onset but with a considerable delay because symptoms are unspecific and less severe, the thrombus might already be isodense, resulting in false-negative imaging findings [7].

Contrast-Enhanced CT

The *empty delta sign* – a direct sign of CVST on contrast-enhanced CT – represents a triangular area of contrast enhancement with a center of relatively low attenuation [67–69]. It is typically found in the superior sagittal sinus. With the wide availability of CTA, the importance of the empty delta sign for the diagnosis of a CVST has decreased.

CTA

According to the latest version of the guidelines of the German Neurological Society, CTA can be regarded as equivalent to venous MRA for the diagnosis of CVST [1]. Multidetector-row CTA (MDCTA) depicts the cerebral veins and sinuses with a high spatial and temporal resolution [42, 70–73], and allows for high-quality multiplanar reconstructions and/or sliding-thin-slab maximum intensity projections [74] (Figure 15). There is upcoming evidence that CTA might be even superior to venous TOF-MRA especially regarding small veins, the inferior

sagittal sinus, and the nondominant transverse sinus [1, 42]. A major advantage of CTA over TOF-MRA is that it is not prone to flow artifacts [42]. Its very short examination time, and the possibility of simultaneous visualization of the cerebral arterial and venous system by application of a single contrast bolus [75] further increase the value of CTA especially in the emergency setting.

On CTA, a venous thrombus is visualized as a contrast filling defect in the respective vessel. Recent studies demonstrated both a sensitivity and a specificity of 100% of MDCTA for ST, compared to MRI as gold standard [42, 76] (Figure 16).

CTA has been shown to depict not only the cerebral sinuses but also the deep cerebral veins in high percentages [42] (Figure 15). However, systematic studies on the value of CTA for the diagnosis of a DCVT are lacking to date. With regard to the cortical veins, there is emerging evidence that MDCTA might be of limited value [13]. Three potential causes of false-negative results on CTA should be considered. (1) In the acute phase, a strongly hyperdense clot ("cord sign" or "dense vein sign") might simulate a regular contrast filling of the respective vessel, and might be a potential source of false-negative results on CTA. To avoid this pitfall, concomitant NECT should always be assessed for the presence of a dense vein sign, especially if interpreting the deep cerebral veins on CTA. (2) A chronic, organized thrombus can show a contrast enhancement and then would not result in a filling defect on CTA. (3) With regard to small veins, partial volume effects from the enhancing vessel walls might obscure the filling defect [42, 67]. Theoretically, prominent arachnoid granulations could also be a source of false-positive results. Yet, there is evidence that they can easily be differentiated from a thrombosis in practice, based on their typical appearance as well-circumscribed, round to ovoid structures

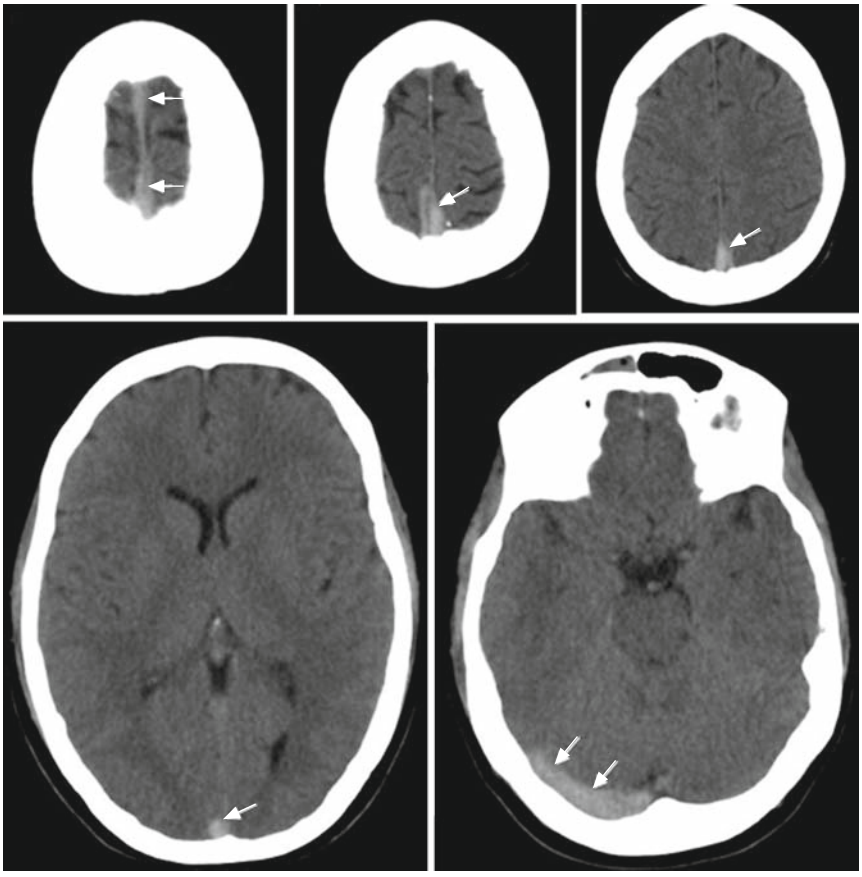

Figure 13. True-positive cord sign in a patient with thrombosis of the superior sagittal sinus and the right transverse sinus (arrows).

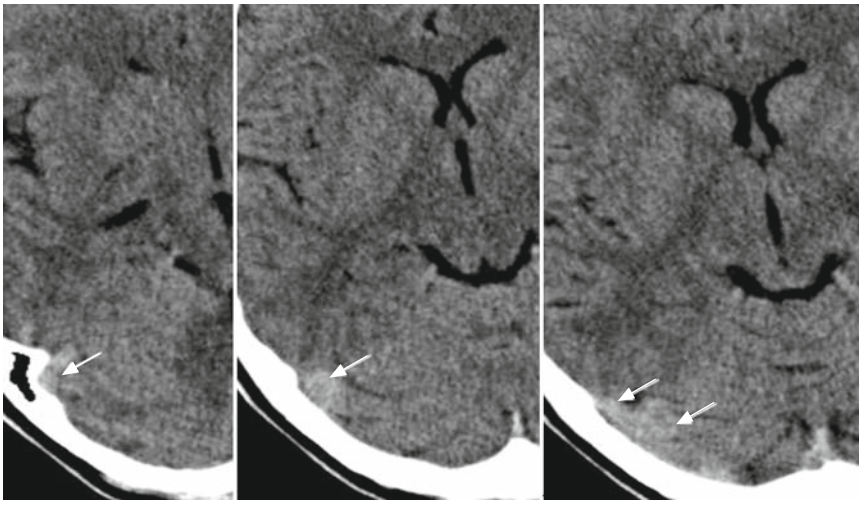

Figure 14. False-positive cord sign in the right transverse sinus (arrows) in a patient without CVST, but with an elevated hematocrit value.

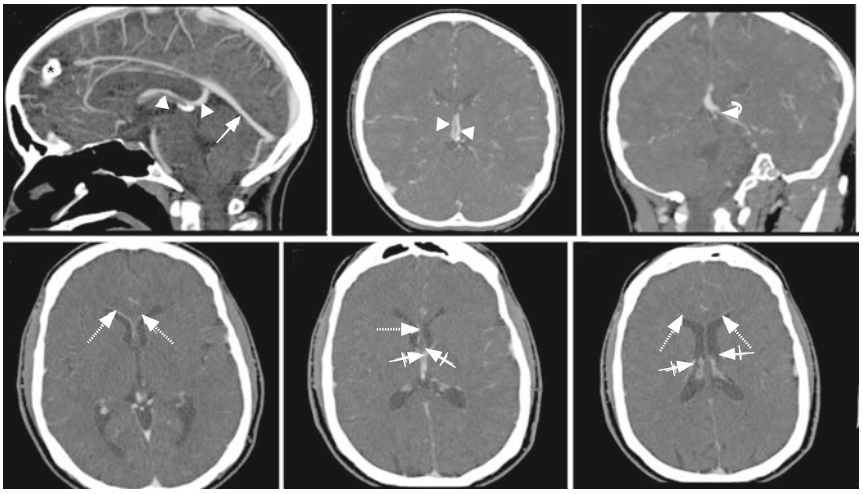

Figure 15. Multiplanar reconstructions of an MDCTA clearly depict the deep cerebral veins and the straight sinus (normal arrows). Arrowheads: internal cerebral veins; dotted arrows: septal veins; curved arrow: basal vein of Rosenthal; crossed arrows: thalamostriate veins. Calcification of the anterior falx (black asterisk) as an additional finding.

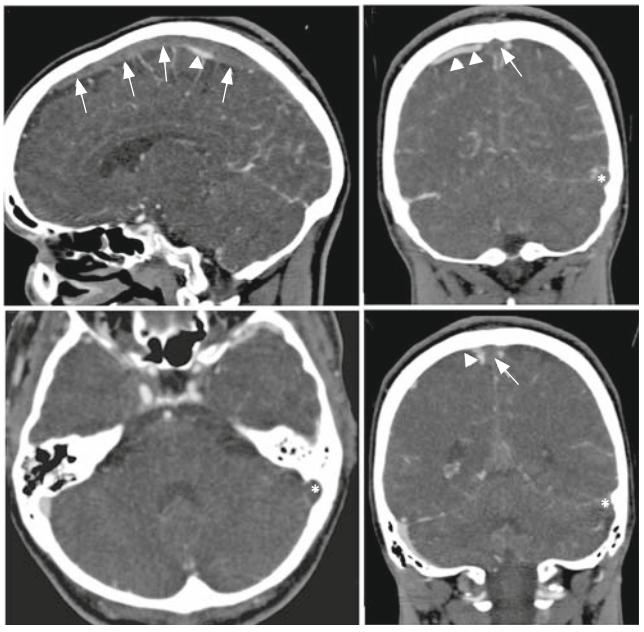

Figure 16. Multiplanar reconstructions of an MDCTA performed in a 29-year-old patient with thrombosis of the superior sagittal sinus (arrows), and the left transverse sinus (asterisks). There is a prominent cortical vein visible (arrowheads). This finding might indicate stagnant flow in an enlarged cortical vein, or just an anatomic variant. This cannot be differentiated based on MDCTA, because there is no dynamic information, as it would be in DSA.

showing the same attenuation as cerebrospinal fluid [42].

The radiation dose represents only a relative drawback of CTA, as it has been shown to be rather low, namely < 1 mSv for an MDCTA performed with 120 kV, which is less than the mean effective dose of an NECT [77].

Conclusion

MRI represents the current gold standard for CVST, and dominates the diagnostic arms of large international trials on this entity. Yet, its interpretation requires expert knowledge of the time- and sequence-dependent clot signal characteristics. This represents a drawback of MRI versus CTA in clinical routine.

MDCTA is a fast, widely accessible, and cost-effective alternative to MRI, and less prone to flow artifacts. For ST, there is evidence that MDCTA is at least equally sensitive compared to venous MRA. Thus, it is especially useful in the emergency setting, or in cases in which MR is not feasible or yields ambiguous results.

NECT alone cannot reliably exclude an ST, but is very sensitive for direct signs of DCVT. Therefore, suspicion of a DCVT should be high, if a dense vein sign is present on NECT.

If an involvement of the cortical veins or an isolated CVT is suspected, MRI with T2*-weighted images are strongly recommended, as all other imaging modalities and MR sequences have a low sensitivity for this entity.

Conflict of Interest Statement

The authors declare that there is no actual or potential conflict of interest in relation to this article.

References

1. Leitlinien für Diagnostik und Therapie in der Neurologie, 4. Aufl. Stuttgart: Thieme, 2008.
2. Linn J, Brückmann H. Differential diagnosis of nontraumatic intracerebral hemorrhage. Clin Neuroradiol 2009;19:45–61.
3. Stam J. Current concepts: Thrombosis of the cerebral veins and sinuses. N Engl J Med 2005;352:1791–8.
4. Coutinho JM, Ferro JM, Canhão P, Barinagarrementeria F, Cantú C, Bousser MG, Stam J. Cerebral venous and sinus thrombosis in women. Stroke 2009;40:2356–61.
5. Ferro JM, Bacelar-Nicolau H, Rodrigues T, Bacelar-Nicolau L, Canhão P, Crassard I, Bousser MG, Dutra AP, Massaro A, Mackowiack-Cordiolani MA, Leys D, Fontes J, Stam J, Barinagarrementeria F, ISCVT and VENOPORT Investigators. Risk score to predict the outcome of patients with cerebral vein and dural sinus thrombosis. Cerebrovasc Dis 2009;28:39–44.

6. Filippidis A, Kapsalaki E, Patramani G, Fountas KN. Cerebral venous sinus thrombosis: review of the demographics, pathophysiology, current diagnosis, and treatment. Neurosurg Focus 2009;27:E3.
7. Annamraju RB, Venkatesan R, Vu AT. T2*-Weighted Angiography (SWAN) : T2*-weighted non-contrast imaging with multi-echo acquisition & reconstruction. Proceedings of the ESMRMB, Valencia, 2.–4. 10.2008: Abstract 482.
8. Ferro JM, Canhão P, Stam J, Bousser MG, Barinagarrementeria F, ISCVT Investigators. Prognosis of cerebral vein and dural sinus thrombosis: results of the International Study on Cerebral Vein and Dural Sinus Thrombosis (ISCVT). Stroke 2004;35:664–70.
9. Canhão P, Ferro JM, Lindgren AG, Bousser MG, Stam J, Barinagarrementeria F, ISCVT Investigators. Causes and predictors of death in cerebral venous thrombosis. Stroke 2005;36:1720–5.
10. Jacobs K, Moulin T, Bogousslavsky J, Woimant F, Dehaene I, Tatu L, Besson G, Assouline E, Casselman J. The stroke syndrome of cortical vein thrombosis. Neurology 1996;47:376–82.
11. Boukobza M, Crassard I, Bousser MG, Chabriat H. MR imaging features of isolated cortical vein thrombosis: diagnosis and follow-up. AJNR Am J Neuroradiol 2009;30:344–8.
12. Sagduyu A, Sirin H, Mulayim S, Bademkiran F, Yunten N, Kitis O, Calli C, Dalbasti T, Kumral E. Cerebral cortical and deep venous thrombosis without sinus thrombosis: clinical MRI correlates. Acta Neurol Scand 2006;114:254–60.
13. Linn J, Michl S, Katja B, Pfefferkorn T, Wiesmann M, Hartz S, Dichgans M, Brückmann H. Cortical vein thrombosis: the diagnostic value of different imaging modalities. Neuroradiology: in press (Epub 2010 Jan 28).
14. Oka K, Rhoton AL Jr, Barry M, Rodriguez R. Microsurgical anatomy of the superficial veins of the cerebrum. Neurosurgery 1985;17:711–48.
15. Renowden S. Cerebral venous sinus thrombosis. Eur Radiol 2004;14: 215–26.
16. Chang R, Friedman DP. Isolated cortical venous thrombosis presenting as subarachnoid hemorrhage: a report of three cases. AJNR Am J Neuroradiol 2004;25:1676–9.
17. Derdeyn CP, Powers WJ. Isolated cortical venous thrombosis and ulcerative colitis. AJNR Am J Neuroradiol 1998;19:488–90.
18. Urban PP, Müller-Forell W. Clinical and neuroradiological spectrum of isolated cortical vein thrombosis. J Neurol 2005;252:1476–81.
19. Fellner FA, Fellner C, Aichner FT, Mölzer G. Importance of T2*-weighted gradient-echo MRI for diagnosis of cortical vein thrombosis. Eur J Radiol 2005;56:235–9.
20. Cakmak S, Hermier M, Montavont A, Derex L, Mauguière F, Trouillas P, Nighoghossian N. T2*SW-weighted MRI in cortical venous thrombosis. Neurology 2004;63:1698.
21. Duncan IC, Fourie PA. Imaging of cerebral isolated cortical vein thrombosis. AJR Am J Roentgenol 2005;184:1317–9.
22. Albayram S, Kara B, Ipek H, Ozbayrak M, Kantarci F. Isolated cortical venous thrombosis associated with intracranial hypotension syndrome. Headache 2009;49:916–9.
23. Rathakrishnan R, Sharma VK, Chan BP. Isolated cortical vein thrombosis in a patient with arteriovenous malformation. J Clin Neurosci 2009;16:856–7.
24. Thamburaj K, Choudhary A. Hyperintense vessel sign: isolated cortical venous thrombosis after L-asparaginase therapy. Pediatr Radiol 2009; 39:757.
25. Einhaupl KM, Villringer A, Meister W, Mehraein S, Garner C, Pellkofer M, Haberl RL, Pfister HW, Schmiedek P. Heparin treatment in sinus venous thrombosis. Lancet 1991;338:597–600.
26. Strupp M, Einhaupl KM, Bousser M-G. Cerebral venous and sinus thrombosis. In: Brandt T, Dichgans J, Caplan LR, eds. Neurological disorders: course and treatment, 2nd edn. San Diego: Academic Press, 2003: 447–60.
27. Ameri A, Bousser MG. Cerebral venous thrombosis. Neurol Clin 1992;10: 87–111.
28. deVeber G, Andrew M, Adams C, Bjornson B, Booth F, Buckley DJ, Camfield CS, David M, Humphreys P, Langevin P, MacDonald EA, Gillett J, Meaney B, Shevell M, Sinclair DB, Yager J, the Canadian Pediatric Ischemic Stroke Study Group. Cerebral sinovenous thrombosis in children. N Engl J Med 2001;345:417–23.
29. Ferro JM, Canhão P, Bousser MG, Stam J, Barinagarrementeria F, ISCVT Investigators. Cerebral vein and dural sinus thrombosis in elderly patients. Stroke 2005;36:1927–32.
30. Ferro JM, Lopes MG, Rosas MJ, Fontes J, VENOPORT Investigators. Delay in hospital admission of patients with cerebral vein and dural sinus thrombosis. Cerebrovasc Dis 2005;19:152–6.
31. Ferro JM, Canhão P. Acute treatment of cerebral venous and dural sinus thrombosis. Curr Treat Options Neurol 2008;10:126–37.
32. Tehindrazanarivelo AD, Bousser MG. Idiopathic intracranial hypertension and cerebral dural sinus thrombosis. Am J Med 1994;97:200–1.
33. Leker RR, Steiner I. Features of dural sinus thrombosis simulating pseudotumour cerebri. Eur J Neurol 1999;6:601–4.
34. Pfefferkorn T, Crassard I, Linn J, Dichgans M, Boukobza M, Bousser MG. Clinical features, course and outcome in deep cerebral venous system thrombosis: an analysis of 32 cases. J Neurol 2009;256:1839–45.
35. Kosinski CM, Mull M, Schwarz M, Koch B, Biniek R, Schlafer J, Milkereit E, Willmes K, Schiefer J. Do normal D-dimer levels reliably exclude cerebral sinus thrombosis? Stroke 2004;35:2820–5.
36. Crassard I, Soria C, Tzourio C, Woimant F, Drouet L, Ducros A, Bousser MG. A negative D-dimer assay does not rule out cerebral venous thrombosis: a series of seventy-three patients. Stroke 2005;36:1716–9.
37. Ferro JM, Canhão P, Stam J, Bousser MG, Barinagarrementeria F, Massaro A, Ducrocq X, Kasner SE, ISCVT Investigators. Delay in the diagnosis of cerebral vein and dural sinus thrombosis: influence on outcome. Stroke 2009;40:3133–8.
38. Girot M, Ferro JM, Canhão P, Stam J, Bousser MG, Barinagarrementeria F, Leys D, ISCVT Investigators. Predictors of outcome in patients with cerebral venous thrombosis and intracerebral hemorrhage. Stroke 2007;38:337–42.
39. Herrmann KA, Sporer B, Yousry TA. Thrombosis of the internal cerebral vein associated with transient unilateral thalamic edema: a case report and review of the literature. AJNR Am J Neuroradiol 2004;25: 1351–5.
40. Lafitte F, Boukobza M, Guichard JP, Hoeffel C, Reizine D, Ille O, Woimant F, Merland JJ. MRI and MRA for diagnosis and follow-up of cerebral venous thrombosis (CVT). Clin Radiol 1997;52:672–9.
41. Teasdale E. Cerebral venous thrombosis: making the most of imaging. J R Soc Med 2000;93:234–7.
42. Linn J, Ertl-Wagner B, Seelos KC, Strupp M, Reiser M, Brückmann H, Brüning R. Diagnostic value of multidetector-row CT angiography in the evaluation of thrombosis of the cerebral venous sinuses. AJNR Am J Neuroradiol 2007;28:946–52.
43. Chang YJ, Huang CC, Wai YY. Isolated cortical venous thrombosis – discrepancy between clinical features and neuroradiologic findings. A case report. Angiology 1995;46:1133–8.
44. Connor SE, Jarosz JM. Magnetic resonance imaging of cerebral venous sinus thrombosis. Clin Radiol 2002;57:449–61.
45. Idbaih A, Boukobza M, Crassard I, Porcher R, Bousser MG, Chabriat H. MRI of clot in cerebral venous thrombosis. High diagnostic value of susceptibility-weighted images. Stroke 2006;37:991–5.
46. Hinman JM, Provenzale JM. Hypointense thrombus on T2-weighted MR imaging: a potential pitfall in the diagnosis of dural sinus thrombosis. Eur J Radiol 2002;41:147–52.
47. Favrole P, Guichard JP, Crassard I, Bousser MG, Chabriat H. Diffusion-weighted imaging of intravascular clots in cerebral venous thrombosis. Stroke 2004;35:99–103.
48. Lövblad KO, Bassetti C, Schneider J, Guzman R, El-Koussy M, Remonda L, Schroth G. Diffusion-weighted mr in cerebral venous thrombosis. Cerebrovasc Dis 2001;11:169–76.

49. Selim M, Fink J, Linfante I, Kumar S, Schlaug G, Caplan LR. Diagnosis of cerebral venous thrombosis with echo-planar T2*-weighted magnetic resonance imaging. Arch Neurol 2002;59:1021–6.
50. Leach JL, Strub WM, Gaskill-Shipley MF. Cerebral venous thrombus signal intensity and susceptibility effects on gradient recalled-echo MR imaging. AJNR Am J Neuroradiol 2007;28:940–5.
51. Linn J, Herms J, Dichgans M, Brückmann H, Fesl G, Freilinger T, Wiesmann M. Subarachnoid hemosiderosis and superficial cortical hemosiderosis in cerebral amyloid angiopathy. AJNR Am J Neuroradiol 2008; 29:184–6.
52. Haacke EM, Xu Y, Cheng YC, Reichenbach JR. Susceptibility weighted imaging (SWI). Magn Reson Med 2004;52:612–8.
53. Annamraju RB, Venkatesan R, Vu AT. T2*-weighted angiography (SWAN): T2*-weighted non-contrast imaging with multi-echo acquisition & reconstruction. Proceedings of the ESMRMB, Valencia, October 2–4, 2008:abstract 482.
54. Kawabori M, Kuroda S, Kudo K, Terae S, Kaneda M, Nakayama N, Iwasaki Y. Susceptibility-weighted magnetic resonance imaging detects impaired cerebral hemodynamics in the superior sagittal sinus thrombosis – case report. Neurol Med Chir (Tokyo) 2009;49:248–51.
55. Ayanzen RH, Bird CR, Keller PJ, McCully FJ, Theobald MR, Heiserman JE. Cerebral MR venography: normal anatomy and potential diagnostic pitfalls. AJNR Am J Neuroradiol 2000;21:74–8.
56. Zhang XL, Qiu SJ, Zhang Y, Zhang YZ, Wen G, Chen B. Phase-contrast magnetic resonance angiography for assessment of intracranial venous sinus lesions. Nan Fang Yi Ke Da Xue Xue Bao 2006;26:1539–42.
57. Lettau M, Sartor K, Heiland S, Hähnel S. 3T high-spatial-resolution contrast-enhanced MR angiography of the intracranial venous system with parallel imaging. AJNR Am J Neuroradiol 2009;30:185–7.
58. Liang L, Korogi Y, Sugahara T, Ikushima I, Shigematsu Y, Takahashi M, Provenzale JM. Normal structures in the intracranial dural sinuses: delineation with 3D contrast-enhanced magnetization prepared rapid acquisition gradient-echo imaging sequence. AJNR Am J Neuroradiol 2002;23:1739–46.
59. Cashen TA, Carr JC, Shin W, Walker MT, Futterer SF, Shaibani A, McCarthy RM, Carroll TJ. Intracranial time-resolved contrast-enhanced MR angiography at 3T. AJNR Am J Neuroradiol 2006;27:822–9.
60. Meckel S, Glücker TM, Kretschmar M, Scheffler K, Radü EW, Wetzel SG. Display of dural sinuses with time-resolved, contrast-enhanced three-dimensional MR venography. Cerebrovasc Dis 2008;25:217–24.
61. Meckel S, Reisinger C, Bremerich J, Damm D, Wolbers M, Engelter S, Scheffler K, Wetzel SG. Cerebral venous thrombosis: diagnostic accuracy of combined, dynamic and static, contrast-enhanced 4D MR venography. AJNR Am J Neuroradiol:in press (Epub 2009 Nov 5).
62. Mullins ME, Grant PE, Wang B, Gonzalez RG, Schaefer PW. Parenchymal abnormalities associated with cerebral venous sinus thrombosis: assessment with diffusion-weighted MR imaging. AJNR Am J Neuroradiol 2004;25:1666–75.
63. Ducreux D, Oppenheim C, Vandamme X, Dormont D, Samson Y, Rancurel G, Cosnard G, Marsault C. Diffusion-weighted imaging patterns of brain damage associated with cerebral venous thrombosis. AJNR Am J Neuroradiol 2001;22:261–8.
64. Forbes KP, Pipe JG, Heiserman JE. Evidence for cytotoxic edema in the pathogenesis of cerebral venous infarction. AJNR Am J Neuroradiol 2001;22:450–5.
65. Srivastava AK, Kalita J, Haris M, Gupta RK, Misra UK. Radiological and histological changes following cerebral venous sinus thrombosis in a rat model. Neurosci Res 2009;65:343–6.
66. Vijay RKP. The cord sign. Radiology 2006;240:299–300.
67. Virapongse C, Cazenave C, Quisling R, Sarwar M, Hunter S. The empty delta sign: frequency and significance in 76 cases of dural sinus thrombosis. Radiology 1987;162:779–85.
68. Provenzale JM, Joseph GJ, Barboriak DP. Dural sinus thrombosis: findings on CT and MR imaging and diagnostic pitfalls. AJR Am J Roentgenol 1998:170:777–83.
69. Lee EJ. The empty delta sign. Radiology 2002;224:788–9.
70. Hagen T, Bartylla K, Waziri A, Schmitz B, Piepgras U. The place of CT angiography in the diagnosis of cerebral sinus thrombosis. Radiologe 1996;36:859–66.
71. Wetzel SG, Kirsch E, Stock KW, Kolbe M, Kaim A, Radue EW. Cerebral veins: comparative study of CT venography with intraarterial digital subtraction angiography. AJNR Am J Neuroradiol 1999;20:249–55.
72. Hunerbein R, Reuter P, Meyer W, Kuhn FP. CT angiography of cerebral venous circulation: anatomical visualization and diagnostic pitfalls in interpretation. Rofo 1997;167:612–8.
73. Klingebiel R, Busch M, Bohner G, Zimmer C, Hoffmann O, Masuhr F. Multi-slice CT angiography in the evaluation of patients with acute cerebrovascular disease – a promising new diagnostic tool. J Neurol 2002;249:43–9.
74. Ertl-Wagner B, Bruening R, Blume J, Hoffmann RT, Mueller-Schunk S, Snyder B, Reiser MF. Relative value of sliding-thin-slab multiplanar reformations and sliding-thin-slab maximum intensity projections as reformatting techniques in multisection CT angiography of the cervicocranial vessels. AJNR Am J Neuroradiol 2006;27:107–13.
75. Klingebiel R, Zimmer C, Rogalla P, Kivelitz D, Bohner G, Götze R, Lehmann R. Assessment of the arteriovenous cerebrovascular system by multi-slice CT. A single-bolus, monophasic protocol. Acta Radiol 2001;42:560–2.
76. Gaikwad AB, Mudalgi BA, Patankar KB, Patil JK, Ghongade DV. Diagnostic role of 64-slice multidetector row CT scan and CT venogram in cases of cerebral venous thrombosis. Emerg Radiol 2008;15:325–33.
77. Ertl-Wagner B, Hoffmann RT., Bruening R, Herrmann K, Snyder B, Blume JD, Reiser MF. Multi-slice CT angiography of the brain at various kilovoltage settings. Radiology 2004;231:528–35.

Address for Correspondence
Jennifer Linn, MD
Department of Neuroradiology
University Hospital Munich
Marchioninistraße 15
81377 Munich
Germany
Phone (+49/89) 7095-2501, Fax -2509
e-mail: linn@nrad.de